

Non-Stoichiometric LaVO₃. II. Powder Neutron Diffraction Study of Crystal and Magnetic Structure for La_{1-x}VO₃, 0.00 ≤ x ≤ 0.10

Helene Seim,^a Helmer Fjellvåg^{a,*} and Bjørn C. Hauback^b

^aDepartment of Chemistry, University of Oslo, N-0315 Oslo 3, Norway and ^bInstitute for Energy Technology, N-2007 Kjeller, Norway

Seim, H., Fjellvåg, H. and Hauback, B. C., 1998. Non-Stoichiometric LaVO₃. II. Powder Neutron Diffraction Study of Crystal and Magnetic Structure for La_{1-x}VO₃, 0.00 ≤ x ≤ 0.10. – Acta Chem. Scand. 52: 1301–1306. © Acta Chemica Scandinavica 1998.

The effect of lanthanum non-stoichiometry on the crystal and magnetic structure of La_{1-x}VO₃ is described on the basis of powder neutron diffraction data. The LaVO₃, La_{0.92}VO₃ and La_{0.90}VO₃ samples were synthesized from citrate precursors with subsequent reduction of the pentavalent vanadium-containing intermediates by zirconium getter or by reductive gas mixtures. Atomic coordinates at 10 and 298 K were deduced from Rietveld-type refinements. La_{1-x}VO₃ takes the orthorhombically distorted GdFeO₃-type variant of the perovskite-type structure. At 298 K, the orthorhombic distortion of the unit cell metric increases with increasing lanthanum deficiency, but there is no major change in atomic coordinates. On cooling, LaVO₃ and La_{0.92}VO₃ undergo first-order magneto-structural phase transitions at 140 ± 1 and 83 ± 1 K, respectively. The ordered antiferromagnetic moment at 10 K is of the C-type, and is lowered from 1.47(4) μ_B for LaVO₃ to 0.83 μ_B for La_{0.92}VO₃. For La_{0.90}VO₃ no structural transition occurs, nor were any signs of magnetic long-range order observed.

The crystal structure, and in particular the correct symmetry at and below room temperature, has repeatedly been debated for LaVO₃. Early reports^{1–6} described the structure at 298 K as a cubic or tetragonal perovskite. However, it is now settled that the structure at 298 K is of the orthorhombic GdFeO₃ type. At low temperatures LaVO₃ undergoes structural and magnetic, probably intimately coupled, transitions, and transition temperatures between 128 and 140 K have been reported.^{2–7} Recently we described the existence of substantial lanthanum non-stoichiometry in La_{1-x}VO₃ and showed that the lanthanum content (and hence the average oxidation state for vanadium) has a strong influence on the low-temperature properties.

Bordet *et al.*⁸ found that early reports on the crystal structure of LaVO₃, in particular below the structural phase transition, were incorrect with respect to crystal symmetry. By using synchrotron X-ray and neutron powder diffraction Bordet *et al.*⁸ described an orthorhombic unit cell for LaVO₃ at 298 K (*a* = 555.5, *b* = 784.4 and *c* = 555.3 pm, space group *Pnma*) which became slightly monoclinically distorted below 140 K; *a* = 559.3, *b* = 775.9 and *c* = 556.4 pm and *γ* = 90.125° at 100 K. In contrast to the orthorhombic model, the monoclinic

model has two non-equivalent V atoms in the unit cell. Support for the latter model has been provided by ⁵¹V NMR data.⁹

Shirakawa *et al.*⁶ reported that in the case of field cooled (FC) samples, the structural phase transition was followed by a magnetic transition into a diamagnetic state. A diamagnetic susceptibility as large as $-2.4 \times 10^{-2} \text{ cm}^3 \text{ mol}^{-1}$ was found for a measuring field of 200 Oe. The observations were in accordance with similar data presented by Mahajan *et al.*⁷ According to Ngyen *et al.*¹⁰ the anomalous diamagnetism is caused by weak ferromagnetism with moment orientation antiparallel to the magnetizing field, where an orbital component is controlling the direction of the spin canting.

Recently, Hartree–Fock band structure calculations of the electronic and orbital ordering in 3d-perovskites have been performed.¹¹ For the LaVO₃ insulator, the calculations show that without any structural distortion or with an *a*-type Jahn–Teller distortion for the d²-ion (V^{III}), C-type antiferromagnetic order would be stable, as actually has been observed by Zubkov *et al.*³ For a d-type Jahn–Teller distortion, like in YVO₃, G-type antiferromagnetic order becomes stable. Presently, the study of the intriguing structural and magnetic properties of LaVO₃ have been extended into the non-stoichiometric range, i.e. La_{1-x}VO₃, 0.00 ≤ x ≤ 0.10. The effects of

* To whom correspondence should be addressed.

lanthanum deficit on the magnetostructural transition and on the crystal and magnetic structure are described on the basis of powder X-ray and neutron diffraction data.

Experimental

Large scale (15 g) powder neutron diffraction samples were synthesized for LaVO_3 , $\text{La}_{0.92}\text{VO}_3$ and $\text{La}_{0.90}\text{VO}_3$ with basis in the citrate method. The La_2O_3 starting material was preheated to 1173 K to remove any hydrated and/or carbonated species. La_2O_3 (99.99% Unocal 76, Molycorp Inc.) was dissolved in 10 ml nitric acid. Thereafter citric acid monohydrate $\text{C}_3\text{H}_4(\text{OH})(\text{COOH})_3 \cdot \text{H}_2\text{O}$ (P.T.Bundi Alarn, Sungai Budi) was gently added. A ratio by weight of 1:25 between La_2O_3 and citric acid was used. The solution was heated until the citric acid was melted and all NO_x gases removed. Finally V_2O_5 (99.5%, Riedel-De-Haen AG) was added and dissolved in the viscous solution. The citrate solution was thereafter dehydrated at 453 K overnight. The formed porous, X-ray amorphous material was then heated at 723 K and the organic components were burned off. The obtained fluffy powders were thereafter treated differently. During heating in air, the stoichiometric sample will form pure LaVO_4 , whereas for lanthanum deficient samples, a vanadium-rich phase, probably V_2O_5 , will form in addition.¹² The desired $\text{La}_{1-x}\text{VO}_3$ samples were finally obtained after a reduction step.

LaVO_3 was obtained by annealing the fluffy powder of the intermediate at 1173 K in air for 20 h, followed by reduction at 1273 K in a tube furnace using a gas mixture of 10% H_2 in N_2/CO_2 with an oxygen partial pressure lower than the required $10^{-12.8}$ bar.¹³ The oxygen partial pressure was monitored with an oxygen sensor (yttrium stabilized zirconia, Dansensor). For the non-stoichiometric samples, a lower annealing temperature for the heating in air is required owing to the low melting point of 943 K for V_2O_5 in the intermediate material. Any larger loss of V_2O_5 was avoided by performing the heat treatment at 843 K for 20 h. The intermediates were subsequently reduced to $\text{La}_{1-x}\text{VO}_3$ at 1273 K in evacuated, closed silica glass ampoules by means of weighed amounts of zirconium (99.5% AD Mackay Inc.) as getter.

Homogeneity and phase purity of the samples were ascertained from powder X-ray diffraction (PXD) at 298 K using Guinier-Hägg cameras ($\text{CuK}\alpha_1$ radiation, Si as internal standard, $a = 543.1061 \text{ pm}^4$). Unit cell dimensions were derived by means of the CELLKANT program.¹⁵ Magnetic susceptibility data were measured by a SQUID magnetometer (MPMS; Quantum Design) for zero field cooled samples and an applied magnetic field of 1 kOe.

Powder neutron diffraction (PND) data were collected at 10 and 298 K with the OPUS IV two-axis diffractometer at the JEEP II reactor, Kjeller. A cylindrical

sample holder was used. Monochromized neutrons of wavelength $\lambda = 182.5 \text{ pm}$ were obtained from reflection from $\text{Ge}(111)$. The scattered intensities were measured by five ^3He detectors, positioned 10° apart. Intensity data were collected between $2\Theta = 10$ and 100° , in steps of $\Delta 2\Theta = 0.05^\circ$. Low temperatures were obtained by means of a Displex cooling system. A Lake Shore DRC 82C controller was used and the temperature was measured and controlled by using a silicon diode. The Hewlett version of the Rietveld program was used to refine atomic coordinates, isotropic displacement factors and magnetic moments.^{16,17} Reflections from Al of the cryostat were excluded prior to the refinements. Free variables in the least-square refinements for data at 298 K included scale factor, three half-width parameters, three unit-cell dimensions, zero point, seven atomic coordinates and three isotropic displacement factors. For the data at 10 K, three additional parameters for the magnetic structure were included. The scattering amplitudes $b_{\text{La}} = 8.24$, $b_{\text{V}} = -0.38$ and $b_{\text{O}} = 5.80 \text{ fm}$, together with the form factor for V^{3+} were used.^{18,19}

Results and discussion

(i) *Crystal structure at 298 K.* The powder neutron diffraction data clearly prove that the GdFeO_3 type variant of the perovskite type structure is retained throughout the entire non-stoichiometric range of $\text{La}_{1-x}\text{VO}_3$. Consistent with the fact that the $x = 0.10$ sample is just outside the homogeneity limit,¹² traces of LaVO_4 were observed in its X-ray and neutron diffraction patterns. $\text{La}_{1-x}\text{VO}_3$ is hence isostructural to LaCrO_3 ²⁰ and one of the three modifications of LaMnO_3 .²¹

Crystal structure data at 298 K are given in Table 1. The unit-cell metric is pseudotetragonal (pseudocubic); however, the orthorhombic distortion in terms of the c/a

Table 1. Unit-cell dimensions and atomic coordinates for $\text{La}_{1-x}\text{VO}_3$ at 298 K derived from Rietveld-type refinements of powder neutron diffraction data.^a

	LaVO_3	$\text{La}_{0.92}\text{VO}_3$	$\text{La}_{0.90}\text{VO}_3$
a/pm	555.18(9)	551.97(8)	551.07(11)
b/pm	784.80(12)	781.43(18)	780.12(24)
c/pm	555.40(9)	553.92(12)	553.71(16)
x_{La}	0.0308(7)	0.0202(9)	0.0167(15)
z_{La}	0.003(2)	0.001(2)	0.008(3)
x_{O1}	0.487(1)	0.489(1)	0.488(2)
z_{O1}	0.082(2)	0.069(2)	0.064(3)
x_{O2}	0.216(1)	0.225(1)	0.226(2)
Y_{O2}	0.5335(8)	0.5338(9)	0.5339(12)
Z_{O2}	0.223(1)	0.226(1)	0.228(2)
R_{n}	2.9	6.4	8.8
R_{p}	7.7	8.8	12.3
R_{exp}	10.0	10.8	12.0

^a Calculated standard deviations in parentheses. Space group $Pnma$, La and O1 in $4(c)$ $x, 1/4, z$; V in $4(b)$ $0, 0, 1/2$ and O2 in $8(d)$ x, y, z . Isotropic displacement factors (in 10^4 pm^2) $B_{\text{La}} = 0.4-0.7$, $B_{\text{V}} = 0.4-0.7$ and $B_{\text{O}} = 0.4-0.9$. Nuclear (R_{n}) and profile (R_{p}) R -factors are given.

ratio increases with increasing La deficit, from 1.0004 for $x=0.00$ to 1.0047 for $x=0.10$. The average, formal oxidation state of vanadium increases from 3.00 in LaVO_3 to 3.30 in $\text{La}_{0.90}\text{VO}_3$. This is reflected in the average V–O bond distance for the rather regular VO_6 octahedron, $d_{\text{av}}(\text{V–O})$ being 200.2 pm for LaVO_3 and 198.0 pm for $\text{La}_{0.90}\text{VO}_3$. This variation is consistent with the calculated increase in bond valence²² from 2.99 for LaVO_3 to 3.16 for $\text{La}_{0.90}\text{VO}_3$ (bond strength parameter 174.3 pm selected for V^{3+}).

(ii) *Phase transition. Crystal and magnetic structure at 10 K.* On cooling, LaVO_3 and $\text{La}_{0.92}\text{VO}_3$ undergo a combined magnetic and structural phase transition. The transition temperatures were determined from the temperature dependence of the integrated intensity of the overlapping (100) and (001) magnetic reflections (Fig. 1). The somewhat poor counting statistics close to the transition suggest that more reliable transition temperatures are provided by magnetic susceptibility data, which give $T_N=140\pm 1$ and 83 ± 1 K, respectively. Consistent with the magnetic susceptibility data, the PND pattern for $\text{La}_{0.90}\text{VO}_3$ at 10 K shows no indication for magnetic long-range order. This implies that T_N drops dramatically with increasing La deficit. According to low-temperature Guinier–Simon X-ray photographs for LaVO_3 ,¹² discontinuous jumps occur in the unit-cell dimensions at the phase transition (at T_t), clearly indicating a first-order nature. The more continuous appearance of the magnetic transition (Fig. 1) suggests that $T_t \leq T_N$, and the observations could well be in line with those reported for CeVO_3 , where $T_t=124 < T_N=136$ K. This

would furthermore be in line with Nguyen and Goodenough, who pointed out that the Jahn–Teller distortion at T_t could only be cooperative below a long-range magnetic ordering temperature (T_N).²³

The magnetostructural distortion is manifested in the b/a axial ratio. For LaVO_3 $b/a=1.4136$ at 298 K (1.414 ideally) and 1.389 at 10 K. For $\text{La}_{0.90}\text{VO}_3$, where no transition occurs, $b/a=1.416$ at 298 K and 1.418 at 10 K. The increasing distortion has been explained by a cooperative Jahn–Teller effect removing the orbital degeneracy of the ${}^3T_{1g}$ configuration of the V^{3+} ion.²³ This variation is evident on consideration of the PND patterns for $\text{La}_{1-x}\text{VO}_3$ at 10 K in Fig. 2. For LaVO_3 line splittings are clearly seen, for $\text{La}_{0.92}\text{VO}_3$ they are less pronounced, whereas for $\text{La}_{0.90}\text{VO}_3$ no splittings are present. Crystal structure data for $\text{La}_{1-x}\text{VO}_3$ at 10 K are given in Table 2; interatomic V–O distances are listed in Table 3.

Bordet *et al.*⁸ described the magnetically ordered LaVO_3 phase as monoclinic, with the γ -angle slightly deviating from 90° , $\gamma=90.125^\circ$ (space group $P2_1/a$). This model was also tested in the present refinements. However, the resolution and statistics of the present data do not allow differentiation between the monoclinic and orthorhombic model. The main difference between these is the non-equivalence between two V sites in the monoclinic structure (Fig. 3) giving rise to stacking of different VO_6 octahedra along the b -axis. The two-site situation may be of importance for the peculiar magnetic temperature–field characteristics of $\text{La}_{1-x}\text{VO}_3$. For field-cooled samples negative magnetization is observed below the magnetostructural phase transition temperature.^{6,7,10,12}

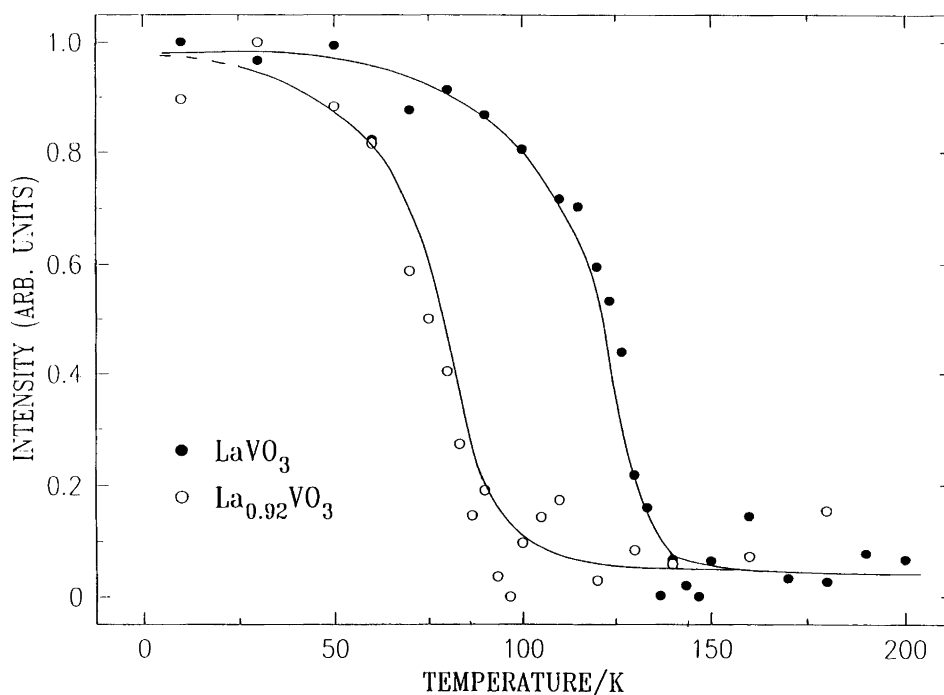


Fig. 1. Temperature dependence of the integrated intensity for the overlapping 100/001 magnetic reflections of LaVO_3 and $\text{La}_{0.92}\text{VO}_3$. Fully drawn lines are given as a guide for the eye.

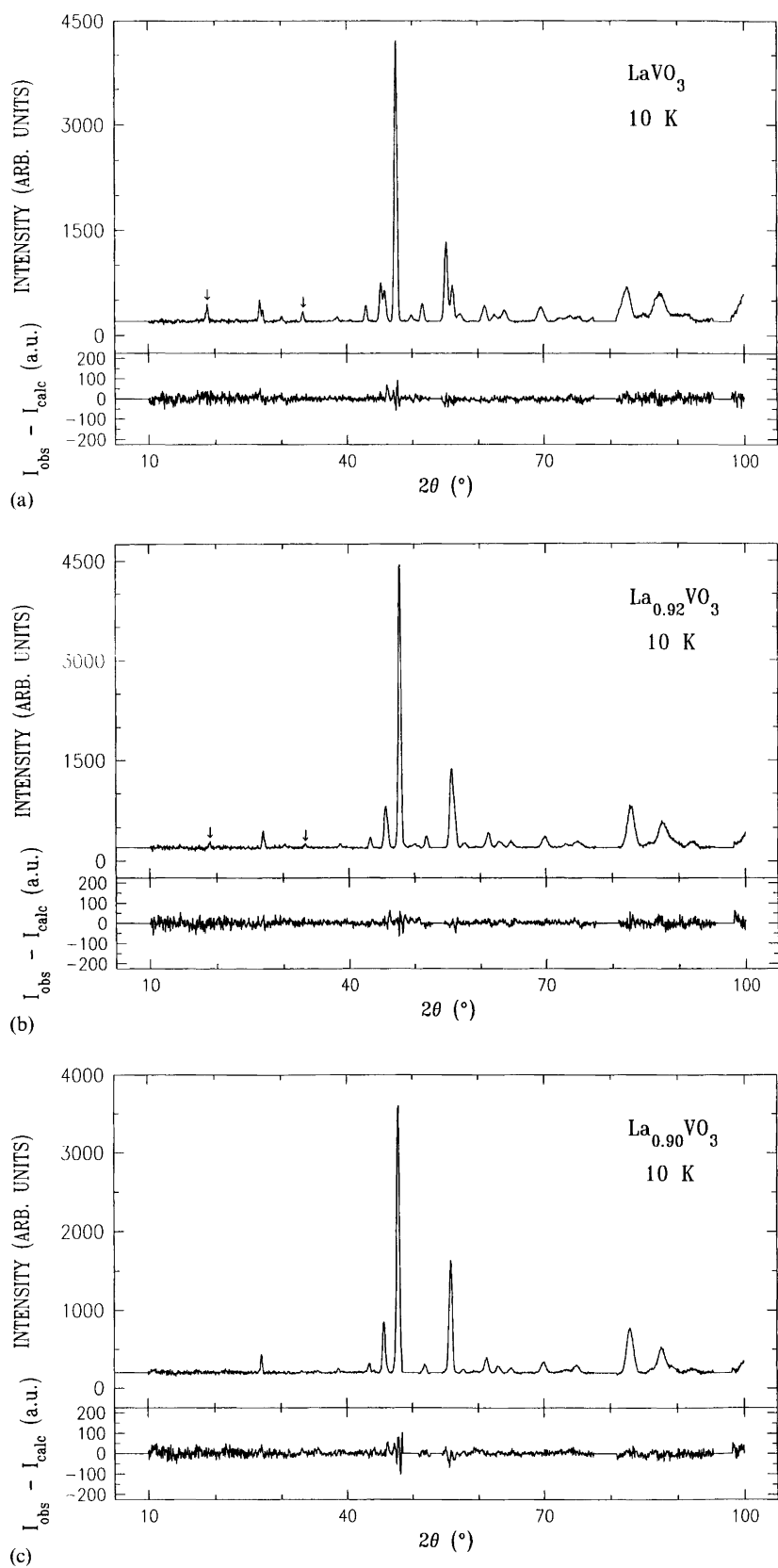


Fig. 2. Observed and difference between observed and calculated powder neutron diffraction pattern for (a) LaVO_3 , (b) $\text{La}_{0.92}\text{VO}_3$ and (c) $\text{La}_{0.90}\text{VO}_3$ at 10 K, $\lambda = 182.5$ pm. Magnetic reflections are marked with arrows.

Table 2. Unit-cell dimensions and atomic coordinates for $\text{La}_{1-x}\text{VO}_3$ at 10 K derived from Rietveld-type refinements of powder neutron diffraction data.^a

	LaVO_3	$\text{La}_{0.92}\text{VO}_3$	$\text{La}_{0.90}\text{VO}_3$
a/pm	558.66(7)	553.07(9)	550.14(12)
b/pm	775.94(7)	776.23(7)	779.93(12)
c/pm	556.18(7)	554.21(9)	552.47(9)
x_{La}	0.0332(5)	0.0262(6)	0.0208(23)
z_{La}	-0.0085(7)(1)	-0.0108(8)	0.003(6)
x_{O1}	0.491(1)	0.491(1)	0.493(3)
z_{O1}	0.0735(6)	0.0710(8)	0.066(5)
x_{O2}	0.2186(8)	0.2213(13)	0.234(4)
y_{O2}	0.5379(3)	0.5336(4)	0.535(3)
z_{O2}	0.2155(8)	0.224(1)	0.219(3)
$\mu_{\text{AF}} (\mu_{\text{B}})$	1.47(4)	0.83(3)	-
R_{n}	3.3	3.6	7.2
R_{m}	13.9	25.6	-
R_{p}	8.4	8.8	12.1
R_{exp}	11.0	11.2	12.4

^aCalculated standard deviations in parentheses. Space group $Pnma$, La and O1 in $4(c)$ $x, 1/4, z$; V in $4(b)$ $0, 0, 1/2$ and O2 in $8(d)$ x, y, z . Isotropic displacement factors (in 10^4 pm^2) $B_{\text{La}}=0.3-0.5$, $B_{\text{V}}=0.2-0.5$ and $B_{\text{O}}=0.3-0.6$. Nuclear (R_{n}), magnetic (R_{m}) and profile (R_{p}) R -factors are given.

Table 3. Interatomic V-O distances (in pm) for VO_6 octahedra in $\text{La}_{1-x}\text{VO}_3$ at 10 K, with uncertainties in parentheses.

	LaVO_3	$\text{La}_{0.92}\text{VO}_3$	$\text{La}_{0.90}\text{VO}_3$
V-O1 ($2\times$)	198.3(1)	198.1(1)	198.4(6)
V-O2 ($2\times$)	199.9(1)	199.8(1)	191.6(6)
V-O2 ($2\times$)	202.0(2)	197.5(2)	203.7(6)
Average	200.0	198.4	197.9

In addition to the explanation proposed by Ngyuyen and Goodenough,¹⁰ one should consider the possibility of different temperature characteristics for the two magnetic V-sublattices like in certain spinels with compensa-

tion points.²⁴ Similar anomalous behaviour has also been found for CeVO_3 ²³ and LaMnO_3 ,²⁵ however, in these cases for zero field cooled samples. For the latter materials no high-resolution diffraction data are at hand, which could provide essential information on the symmetry of the low-temperature phase.

Additional peaks of magnetic origin are marked in the diffraction patterns for LaVO_3 and $\text{La}_{0.92}\text{VO}_3$ at 10 K in Fig. 2. For $\text{La}_{0.92}\text{VO}_3$ the magnetic reflections are rather weak, whereas no indication for any magnetic long range order could be found for $\text{La}_{0.90}\text{VO}_3$. The magnetic moment decreases from $1.47 \mu_{\text{B}}$ for LaVO_3 to $0.83 \mu_{\text{B}}$ for $\text{La}_{0.92}\text{VO}_3$ (Table 2). The magnetic structure of $\text{La}_{1-x}\text{VO}_3$ is of C-type (Fig. 3). Owing to the closeness of the a - and c -axes in length, one could not distinguish between C_x or C_z arrangements.

The orthorhombic rare-earth vanadites, REVO_3 , are all antiferromagnetic. Those with $\text{RE}=\text{La}-\text{Dy}$ exhibit C-type ordering (no data available for Sm, Eu, Gd), those with $\text{RE}=\text{Ho}-\text{Lu}$ have G-type ordering.³ According to Zubkov *et al.*²⁶ most of these compounds exhibit also weak ferromagnetism. The antiferromagnetic ordering temperature decreases with diminishing size of the RE-element,³ from $T_{\text{N}}=140 \text{ K}$ for $\text{RE}=\text{La}$ to $T_{\text{N}}=101 \text{ K}$ for $\text{RE}=\text{Lu}$. A similar variation throughout the RE series is also found for the orthomanganites and orthoferrites of the GdFeO_3 type. This probably results from weakening of magnetic interaction consequent upon mismatch in size between the RE and the transition element, which in turn causes increased deviation in the M-O-M angle from 180° . The drastic reduction in T_{N} for $\text{La}_{1-x}\text{VO}_3$ on increasing the La deficit is not correlated with such changes in the V-O-V angles. The situation appears more likely to be connected with a change in average V-valence. For $\text{La}_{0.90}\text{VO}_3$ magnetic susceptibility data indicate a substantial paramagnetic

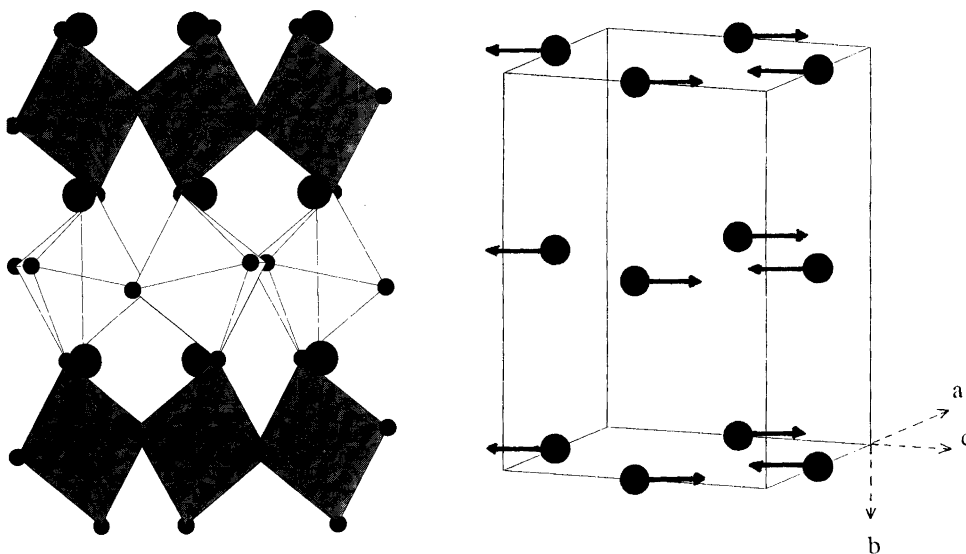


Fig. 3. Monoclinic structure model for LaVO_3 at 10 K. Non-equivalent VO_6 octahedra are shown in different shadings (left), ordering of magnetic moments (right).

moment; however, no magnetic order and no (magneto-) structural phase transition occur for this composition with formally 30% V^{IV}. In this respect the behaviour appears analogous to that observed for non-stoichiometric LaMnO_{3+δ} where the amount of Mn^{IV} can be tuned between 0 and some 35%. Whereas, e.g., LaMnO₃ (0% Mn^{IV}) orders antiferromagnetically below 135 K, LaMnO_{3.08} (16% Mn^{IV}) ferromagnetically below 125 K and La_{0.96}MnO_{3.05} (22% Mn^{IV}) ferromagnetically below 213 K, all with large magnetic moments (2.5–4 μ_B), powder neutron diffraction data for LaMnO_{3.15} (30% Mn^{IV}) show no indication for magnetic long-range order, and a spin-glass situation is proposed.²⁵ The La_{1-x}VO₃ and LaMnO_{3+δ} phases have thus two interesting features in common, (i) weakening of the Jahn–Teller distortion on increasing amounts of tetravalent species and (ii) lack of cooperative magnetic order for M^{III}/M^{IV} ratios around 2:1.

Acknowledgement. Financial support from Norsk Hydro A/S and the Research Council of Norway is gratefully acknowledged.

References

- Kestigan, M., Dickinson, J. G. and Ward, R. *J. Am. Chem. Soc.* **79** (1957) 5598.
- Rogers, D. B., Ferretti, A., Ridgley, D. H., Arnott, R. J. and Goodenough, J. B. *J. Appl. Phys.* **37** (1966) 1431.
- Zubkov, V. G., Bazuev, G. V. and Shveikin, G. P. *Sov. Phys. Solid State* **18** (1976) 1165.
- Sakai, T., Adachi, G., Shiokawa, J. and Shin-ike, T. *J. Appl. Phys.* **48** (1977) 379.
- Mahajan, A. V., Johnston, D. C., Torgeson, D. R. and Borsa, F. *Phys. Rev. B* **46** (1992) 10966.
- Shirakawa, N. and Ishikawa, M. *Jpn. J. Appl. Phys.* **30** (1991) L 755.
- Mahajan, A. V., Johnston, D. C., Torgeson, D. R. and Borsa, F. *Physica C* **185–189** (1991) 1195.
- Bordet, P., Chaillout, C., Marezio, M., Huang, Q., Santoro, A., Cheong, S. W., Takagi, H., Oglesby, C. S. and Batlogg, B. *J. Solid State Chem.* **106** (1993) 253.
- Kikuchi, J., Yasuoka, H., Kokubo, Y. and Ueda, Y. *J. Phys. Soc. Jpn.* **63** (1994) 3577.
- Nguyen, H. C. and Goodenough, J. B. *Phys. Rev. B* **52** (1995) 324.
- Mizokawa, T. and Fujimori, A. *Phys. Rev. B* **54** (1996) 5368.
- Seim, H. and Fjellvåg, H. *Acta Chem. Scand.* **52** (1998) 1096.
- Nakamura, T., Petzow, G. and Gauckler, L. J. *Mater. Res. Bull.* **14** (1979) 649.
- Deslattes, R. D. and Henins, A. *Phys. Rev. Lett.* **31** (1973) 979.
- Ersson, N. O. *CELLKANT Program*, University of Uppsala, Sweden 1981.
- Rietveld, H. M. *J. Appl. Crystallogr.* **2** (1969) 65.
- Hewat, A. W. *UKAERE Harwell Report RRL 73/897*, 1973.
- Sears, V. F. *Neutron News* **3** (1992) 26.
- Watson, R. E. and Freeman, A. J., *Acta Crystallogr.* **14** (1961) 27.
- Geller, S. *Acta Crystallogr.* **10** (1957) 243.
- Elemans, J. B. A. A., van Laar, B., van der Veen, K. R. and Loopstra, B. O. *J. Solid State Chem.* **3** (1971) 238.
- Brese, N. E. and O'Keeffe, M. *Acta Crystallogr., Sect. B* **47** (1991) 92.
- Nguyen, H. C. and Goodenough, J. B. *J. Solid State Chem.* **119** (1995) 24.
- Menyuk, N., Dwight, K. and Wickham, D. G. *Phys. Rev. Lett.* **4** (1960) 119.
- Hauback, B. C., Fjellvåg, H. and Sakai, N. *J. Solid State Chem.* **124** (1996) 43.
- Zubkov, V. G., Bazuev, G. V., Belousov, E. I. and Shveikin, G. P. *Sov. Phys. Solid State* **17** (1975) 193.

Received April 22, 1998.